Letter

# Observation of $\psi(3770) \to \eta J/\psi$

M. Ablikim,[1] M. N. Achasov,[10,b] P. Adlarson,[69] S. Ahmed,[15] M. Albrecht,[4] R. Aliberti,[29] A. Amoroso,[68a,68c] M. R. An,[33] Q. An,[65,51] X. H. Bai,[59] Y. Bai,[50] O. Bakina,[30] R. Baldini Ferroli,[24a] I. Balossino,[25a] Y. Ban,[40,g] V. Batozskaya,[1,38] D. Becker,[29] K. Begzsuren,[27] N. Berger,[29] M. Bertani,[24a] D. Bettoni,[25a] F. Bianchi,[68a,68c] J. Bloms,[62] A. Bortone,[68a,68c] I. Boyko,[30] R. A. Briere,[5] A. Brueggemann,[62] H. Cai,[70] X. Cai,[1,51] A. Calcaterra,[24a] G. F. Cao,[1,56] N. Cao,[1,56] S. A. Cetin,[55a] J. F. Chang,[1,51] W. L. Chang,[1,56] G. Chelkov,[30,a] C. Chen,[37] G. Chen,[1] H. S. Chen,[1,56] M. L. Chen,[1,51] S. J. Chen,[36] T. Chen,[1] X. R. Chen,[26,56] X. T. Chen,[1] Y. B. Chen,[1,51] Z. J. Chen,[21,h] W. S. Cheng,[68c] G. Cibinetto,[25a] F. Cossio,[68c] J. J. Cui,[43] H. L. Dai,[1,51] J. P. Dai,[72] A. Dbeyssi,[15] R. E. de Boer,[4] D. Dedovich,[30] Z. Y. Deng,[1] A. Denig,[29] I. Denysenko,[30] M. Destefanis,[68a,68c] F. De Mori,[68a,68c] Y. Ding,[34] J. Dong,[1,51] L. Y. Dong,[1,56] M. Y. Dong,[1,51,56] X. Dong,[70] S. X. Du,[74] P. Egorov,[30,a] Y. L. Fan,[70] J. Fang,[1,51] S. S. Fang,[1,56] Y. Fang,[1] R. Farinelli,[25a] L. Fava,[68b,68c] F. Feldbauer,[4] G. Felici,[24a] C. Q. Feng,[65,51] J. H. Feng,[52] K. Fischer,[63] M. Fritsch,[4] C. D. Fu,[1] H. Gao,[56] Y. N. Gao,[40,g] Yang Gao,[65,51] I. Garzia,[25a,25b] P. T. Ge,[70] Z. W. Ge,[36] C. Geng,[52] E. M. Gersabeck,[60] A. Gilman,[63] K. Goetzen,[11] L. Gong,[34æ] W. X. Gong,[1,51] W. Gradl,[29] M. Greco,[68a,68c] L. M. Gu,[36] M. H. Gu,[1,51] Y. T. Gu,[13] C. Y. Guan,[1,56] A. Q. Guo,[26,56] L. B. Guo,[35] R. P. Guo,[42] Y. P. Guo,[9,f] A. Guskov,[30,a] T. T. Han,[43] W. Y. Han,[33] X. Q. Hao,[16] F. A. Harris,[58] K. K. He,[48] K. L. He,[1,56] F. H. Heinsius,[4] C. H. Heinz,[29] Y. K. Heng,[1,51,56] C. Herold,[53] M. Himmelreich,[11,d] T. Holtmann,[4] G. Y. Hou,[1,56] Y. R. Hou,[56] Z. L. Hou,[1] H. M. Hu,[1,56] J. F. Hu,[49,i] T. Hu,[1,51,56] Y. Hu,[1] G. S. Huang,[65,51] K. X. Huang,[52] L. Q. Huang,[26,56] L. Q. Huang,[66] X. T. Huang,[43] Y. P. Huang,[1] Z. Huang,[40,g] T. Hussain,[67] N. Hüsken,[23,29] W. Imoehl,[23] M. Irshad,[65,51] J. Jackson,[23] S. Jaeger,[4] S. Janchiv,[27] Q. Ji,[1] Q. P. Ji,[16] X. B. Ji,[1,56] X. L. Ji,[1,51] Y. Y. Ji,[43] H. B. Jiang,[43] S. S. Jiang,[33] X. S. Jiang,[1,51,56] Y. Jiang,[56] J. B. Jiao,[43] Z. Jiao,[19] S. Jin,[36] Y. Jin,[59] M. Q. Jing,[1,56] T. Johansson,[69] N. Kalantar-Nayestanaki,[57] X. S. Kang,[34] R. Kappert,[57] M. Kavatsyuk,[57] B. C. Ke,[74] I. K. Keshk,[4] A. Khoukaz,[62] P. Kiese,[29] R. Kiuchi,[1] R. Kliemt,[11] L. Koch,[31] O. B. Kolcu,[55a] B. Kopf,[4] M. Kuemmel,[4] M. Kuessner,[4] A. Kupsc,[38,69] W. Kühn,[31] J. J. Lane,[60] J. S. Lange,[31] P. Larin,[15] A. Lavania,[22] L. Lavezzi,[68a,68c] Z. H. Lei,[65,51] H. Leithoff,[29] M. Lellmann,[29] T. Lenz,[29] C. Li,[37] C. Li,[41] C. H. Li,[33] Cheng Li,[65,51] D. M. Li,[74] F. Li,[1,51] G. Li,[1] H. Li,[45] H. Li,[65,51] H. B. Li,[1,56] H. J. Li,[16] H. N. Li,[49,i] J. Q. Li,[4] J. S. Li,[52] J. W. Li,[43] Ke Li,[1] L. J. Li,[1] L. K. Li,[1] Lei Li,[3] M. H. Li,[37] P. R. Li,[32,j,k] S. X. Li,[9] S. Y. Li,[54] T. Li,[43] W. D. Li,[1,56] W. G. Li,[1] X. H. Li,[65,51] X. L. Li,[43] Xiaoyu Li,[1,56] Z. Y. Li,[52] H. Liang,[65,51] H. Liang,[1,56] H. Liang,[28] Y. F. Liang,[47] Y. T. Liang,[26,56] G. R. Liao,[12] L. Z. Liao,[43] J. Libby,[22] A. Limphirat,[53] C. X. Lin,[52] D. X. Lin,[26,56] T. Lin,[1] B. J. Liu,[1] C. X. Liu,[1] D. Liu,[15,65] F. H. Liu,[46] Fang Liu,[1] Feng Liu,[6] G. M. Liu,[49,i] H. B. Liu,[13] H. M. Liu,[1,56] Huanhuan Liu,[1] Huihui Liu,[17] J. B. Liu,[65,51] J. L. Liu,[66] J. Y. Liu,[1,56] K. Liu,[1] K. Y. Liu,[34] Ke Liu,[18] L. Liu,[65,51] Lu Liu,[37] M. H. Liu,[9,f] P. L. Liu,[1] Q. Liu,[56] S. B. Liu,[65,51] T. Liu,[9,f] W. K. Liu,[37] W. M. Liu,[65,51] X. Liu,[32,j,k] Y. Liu,[32,j,k] Y. B. Liu,[37] Z. A. Liu,[1,51,56] Z. Q. Liu,[43] X. C. Lou,[1,51,56] F. X. Lu,[52] H. J. Lu,[19] J. G. Lu,[1,51] X. L. Lu,[1] Y. Lu,[1] Y. P. Lu,[1,51] Z. H. Lu,[1] C. L. Luo,[35] M. X. Luo,[73] T. Luo,[9,f] X. L. Luo,[1,51] X. R. Lyu,[56] Y. F. Lyu,[37] F. C. Ma,[34] H. L. Ma,[1] L. L. Ma,[43] M. M. Ma,[1,56] Q. M. Ma,[1] R. Q. Ma,[1,56] R. T. Ma,[56] X. Y. Ma,[1,51] Y. Ma,[40,g] F. E. Maas,[15] M. Maggiora,[68a,68c] S. Maldaner,[4] S. Malde,[63] Q. A. Malik,[67] A. Mangoni,[24b] Y. J. Mao,[40,g] Z. P. Mao,[1] S. Marcello,[68a,68c] Z. X. Meng,[59] J. G. Messchendorp,[57,11] G. Mezzadri,[25a] H. Miao,[1] T. J. Min,[36] R. E. Mitchell,[23] X. H. Mo,[1,51,56] N. Yu. Muchnoi,[10,b] H. Muramatsu,[61] S. Nakhoul,[11,d] Y. Nefedov,[30] F. Nerling,[11,d] I. B. Nikolaev,[10,b] Z. Ning,[1,51] S. Nisar,[8,l] Y. Niu,[43] S. L. Olsen,[56] Q. Ouyang,[1,51,56] S. Pacetti,[24b,24c] X. Pan,[9,f] Y. Pan,[60] A. Pathak,[28] M. Pelizaeus,[4] H. P. Peng,[65,51] K. Peters,[11,d] J. L. Ping,[35] R. G. Ping,[1,56] S. Plura,[29] S. Pogodin,[30] R. Poling,[61] V. Prasad,[65,51] H. Qi,[65,51] H. R. Qi,[54] M. Qi,[36] T. Y. Qi,[9,f] S. Qian,[1,51] W. B. Qian,[56] Z. Qian,[52] C. F. Qiao,[56] J. J. Qin,[66] L. Q. Qin,[12] X. P. Qin,[9,f] X. S. Qin,[43] Z. H. Qin,[1,51] J. F. Qiu,[1] S. Q. Qu,[54] K. H. Rashid,[67] K. Ravindran,[22] C. F. Redmer,[29] K. J. Ren,[33] A. Rivetti,[68c] V. Rodin,[57] M. Rolo,[68c] G. Rong,[1,56] Ch. Rosner,[15] A. Sarantsev,[30,c] Y. Schelhaas,[29] C. Schnier,[4] K. Schoenning,[69] M. Scodeggio,[25a,25b] K. Y. Shan,[9,f] W. Shan,[20] X. Y. Shan,[65,51] J. F. Shangguan,[48] L. G. Shao,[1,56] M. Shao,[65,51] C. P. Shen,[9,f] H. F. Shen,[1,56] X. Y. Shen,[1,56] B. A. Shi,[56] H. C. Shi,[65,51] R. S. Shi,[1,56] X. Shi,[1,51] X. D. Shi,[65,51] J. J. Song,[16] W. M. Song,[28,1] Y. X. Song,[40,g] S. Sosio,[68a,68c] S. Spataro,[68a,68c] F. Stieler,[29] K. X. Su,[70] P. P. Su,[48] Y. J. Su,[56] G. X. Sun,[1] H. Sun,[56] H. K. Sun,[1] J. F. Sun,[16] L. Sun,[70] S. S. Sun,[1,56] T. Sun,[1,56] W. Y. Sun,[28] X. Sun,[21,h] Y. J. Sun,[65,51] Y. Z. Sun,[1] Z. T. Sun,[43] Y. H. Tan,[70] Y. X. Tan,[65,51] C. J. Tang,[47] G. Y. Tang,[1] J. Tang,[52] L. Y. Tao,[66] Q. T. Tao,[21,h] J. X. Teng,[65,51] V. Thoren,[69] W. H. Tian,[45] Y. Tian,[26,56] I. Uman,[55b] B. Wang,[1] B. L. Wang,[56] C. W. Wang,[36] D. Y. Wang,[40,g] F. Wang,[66] H. J. Wang,[32,j,k] H. P. Wang,[1,56] K. Wang,[1,51] L. L. Wang,[1] M. Wang,[43] M. Z. Wang,[40,g] Meng Wang,[1,56] S. Wang,[12] S. Wang,[9,f] T. Wang,[9,f] T. J. Wang,[37] W. Wang,[52] W. H. Wang,[70] W. P. Wang,[65,51] X. Wang,[40,g] X. F. Wang,[32,j,k] X. L. Wang,[9,f] Y. D. Wang,[39] Y. F. Wang,[1,51,56] Y. H. Wang,[41] Y. Q. Wang,[1] Z. Wang,[1,51] Z. Y. Wang,[1,56] Ziyi Wang,[56] D. H. Wei,[12] F. Weidner,[62] S. P. Wen,[1] D. J. White,[60] U. Wiedner,[4] G. Wilkinson,[63] M. Wolke,[69] L. Wollenberg,[4] J. F. Wu,[1,56] L. H. Wu,[1] L. J. Wu,[1,56] X. Wu,[9,f] X. H. Wu,[28] Y. Wu,[65] Y. J. Wu,[26] Z. Wu,[1,51] L. Xia,[65,51] T. Xiang,[40,g] G. Y. Xiao,[36] H. Xiao,[9,f] S. Y. Xiao,[1] Y. L. Xiao,[9,f] Z. J. Xiao,[35] C. Xie,[36] X. H. Xie,[40,g] Y. Xie,[43] Y. G. Xie,[1,51] Y. H. Xie,[6] Z. P. Xie,[65,51] T. Y. Xing,[1,56] C. F. Xu,[1] C. J. Xu,[52] G. F. Xu,[1] H. Y. Xu,[59] Q. J. Xu,[14] X. P. Xu,[48] Y. C. Xu,[56] Z. P. Xu,[36] F. Yan,[9,f] L. Yan,[9,f]

W. B. Yan,[65,51] W. C. Yan,[74] H. J. Yang,[44,e] H. X. Yang,[1] L. Yang,[45] S. L. Yang,[56] Y. X. Yang,[1,56] Yifan Yang,[1,56] Zhi Yang,[26] M. Ye,[1,51] M. H. Ye,[7] J. H. Yin,[1] Z. Y. You,[52] B. X. Yu,[1,51,56] C. X. Yu,[37] G. Yu,[1,56] J. S. Yu,[21,h] T. Yu,[66] C. Z. Yuan,[1,56] L. Yuan,[2] S. C. Yuan,[1] X. Q. Yuan,[1] Y. Yuan,[1,56] Z. Y. Yuan,[52] C. X. Yue,[33] A. A. Zafar,[67] F. R. Zeng,[43] X. Zeng,[6] Y. Zeng,[21,h] Y. H. Zhan,[52] A. Q. Zhang,[1] B. L. Zhang,[1] B. X. Zhang,[1] G. Y. Zhang,[16] H. Zhang,[65] H. H. Zhang,[52] H. H. Zhang,[28] H. Y. Zhang,[1,51] J. L. Zhang,[71] J. Q. Zhang,[35] J. W. Zhang,[1,51,56] J. Y. Zhang,[1] J. Z. Zhang,[1,56] Jianyu Zhang,[1,56] Jiawei Zhang,[1,56] L. M. Zhang,[54] L. Q. Zhang,[52] Lei Zhang,[36] P. Zhang,[1] Q. Y. Zhang,[33,74] Shuihan Zhang,[1,56] Shulei Zhang,[21,h] X. D. Zhang,[39] X. M. Zhang,[1] X. Y. Zhang,[43] X. Y. Zhang,[48] Y. Zhang,[63] Y. T. Zhang,[74] Y. H. Zhang,[1,51] Yan Zhang,[65,51] Yao Zhang,[1] Z. H. Zhang,[1] Z. Y. Zhang,[37] Z. Y. Zhang,[70] G. Zhao,[1] J. Zhao,[33] J. Y. Zhao,[1,56] J. Z. Zhao,[1,51] Lei Zhao,[65,51] Ling Zhao,[1] M. G. Zhao,[37] Q. Zhao,[1] S. J. Zhao,[74] Y. B. Zhao,[1,51] Y. X. Zhao,[26,56] Z. G. Zhao,[65,51] A. Zhemchugov,[30,a] B. Zheng,[66] J. P. Zheng,[1,51] Y. H. Zheng,[56] B. Zhong,[35] C. Zhong,[66] X. Zhong,[52] H. Zhou,[43] L. P. Zhou,[1,56] X. Zhou,[70] X. K. Zhou,[56] X. R. Zhou,[65,51] X. Y. Zhou,[33] Y. Z. Zhou,[9,f] J. Zhu,[37] K. Zhu,[1] K. J. Zhu,[1,51,56] L. X. Zhu,[56] S. H. Zhu,[64] S. Q. Zhu,[36] T. J. Zhu,[71] W. J. Zhu,[9,f] Y. C. Zhu,[65,51] Z. A. Zhu,[1,56] B. S. Zou,[1] and J. H. Zou[1]

(BESIII Collaboration)

[1]*Institute of High Energy Physics, Beijing 100049, People's Republic of China*
[2]*Beihang University, Beijing 100191, People's Republic of China*
[3]*Beijing Institute of Petrochemical Technology, Beijing 102617, People's Republic of China*
[4]*Bochum Ruhr-University, D-44780 Bochum, Germany*
[5]*Carnegie Mellon University, Pittsburgh, Pennsylvania 15213, USA*
[6]*Central China Normal University, Wuhan 430079, People's Republic of China*
[7]*China Center of Advanced Science and Technology, Beijing 100190, People's Republic of China*
[8]*COMSATS University Islamabad, Lahore Campus, Defence Road, Off Raiwind Road, 54000 Lahore, Pakistan*
[9]*Fudan University, Shanghai 200433, People's Republic of China*
[10]*G.I. Budker Institute of Nuclear Physics SB RAS (BINP), Novosibirsk 630090, Russia*
[11]*GSI Helmholtzcentre for Heavy Ion Research GmbH, D-64291 Darmstadt, Germany*
[12]*Guangxi Normal University, Guilin 541004, People's Republic of China*
[13]*Guangxi University, Nanning 530004, People's Republic of China*
[14]*Hangzhou Normal University, Hangzhou 310036, People's Republic of China*
[15]*Helmholtz Institute Mainz, Staudinger Weg 18, D-55099 Mainz, Germany*
[16]*Henan Normal University, Xinxiang 453007, People's Republic of China*
[17]*Henan University of Science and Technology, Luoyang 471003, People's Republic of China*
[18]*Henan University of Technology, Zhengzhou 450001, People's Republic of China*
[19]*Huangshan College, Huangshan 245000, People's Republic of China*
[20]*Hunan Normal University, Changsha 410081, People's Republic of China*
[21]*Hunan University, Changsha 410082, People's Republic of China*
[22]*Indian Institute of Technology Madras, Chennai 600036, India*
[23]*Indiana University, Bloomington, Indiana 47405, USA*
[24a]*INFN Laboratori Nazionali di Frascati, I-00044, Frascati, Italy*
[24b]*INFN Sezione di Perugia, I-06100, Perugia, Italy*
[24c]*University of Perugia, I-06100, Perugia, Italy*
[25a]*INFN Sezione di Ferrara, I-44122, Ferrara, Italy*
[25b]*University of Ferrara, I-44122, Ferrara, Italy*
[26]*Institute of Modern Physics, Lanzhou 730000, People's Republic of China*
[27]*Institute of Physics and Technology, Peace Avenue 54B, Ulaanbaatar 13330, Mongolia*
[28]*Jilin University, Changchun 130012, People's Republic of China*
[29]*Johannes Gutenberg University of Mainz, Johann-Joachim-Becher-Weg 45, D-55099 Mainz, Germany*
[30]*Joint Institute for Nuclear Research, 141980 Dubna, Moscow region, Russia*
[31]*Justus-Liebig-Universitaet Giessen, II. Physikalisches Institut, Heinrich-Buff-Ring 16, D-35392 Giessen, Germany*
[32]*Lanzhou University, Lanzhou 730000, People's Republic of China*
[33]*Liaoning Normal University, Dalian 116029, People's Republic of China*
[34]*Liaoning University, Shenyang 110036, People's Republic of China*
[35]*Nanjing Normal University, Nanjing 210023, People's Republic of China*
[36]*Nanjing University, Nanjing 210093, People's Republic of China*
[37]*Nankai University, Tianjin 300071, People's Republic of China*
[38]*National Centre for Nuclear Research, Warsaw 02-093, Poland*
[39]*North China Electric Power University, Beijing 102206, People's Republic of China*

[40]*Peking University, Beijing 100871, People's Republic of China*
[41]*Qufu Normal University, Qufu 273165, People's Republic of China*
[42]*Shandong Normal University, Jinan 250014, People's Republic of China*
[43]*Shandong University, Jinan 250100, People's Republic of China*
[44]*Shanghai Jiao Tong University, Shanghai 200240, People's Republic of China*
[45]*Shanxi Normal University, Linfen 041004, People's Republic of China*
[46]*Shanxi University, Taiyuan 030006, People's Republic of China*
[47]*Sichuan University, Chengdu 610064, People's Republic of China*
[48]*Soochow University, Suzhou 215006, People's Republic of China*
[49]*South China Normal University, Guangzhou 510006, People's Republic of China*
[50]*Southeast University, Nanjing 211100, People's Republic of China*
[51]*State Key Laboratory of Particle Detection and Electronics, Beijing 100049, Hefei 230026, People's Republic of China*
[52]*Sun Yat-Sen University, Guangzhou 510275, People's Republic of China*
[53]*Suranaree University of Technology, University Avenue 111, Nakhon Ratchasima 30000, Thailand*
[54]*Tsinghua University, Beijing 100084, People's Republic of China*
[55a]*Turkish Accelerator Center Particle Factory Group, Istinye University, 34010, Istanbul, Turkey*
[55b]*Near East University, Nicosia, North Cyprus, Mersin 10, Turkey*
[56]*University of Chinese Academy of Sciences, Beijing 100049, People's Republic of China*
[57]*University of Groningen, NL-9747 AA Groningen, Netherlands*
[58]*University of Hawaii, Honolulu, Hawaii 96822, USA*
[59]*University of Jinan, Jinan 250022, People's Republic of China*
[60]*University of Manchester, Oxford Road, Manchester, M13 9PL, United Kingdom*
[61]*University of Minnesota, Minneapolis, Minnesota 55455, USA*
[62]*University of Muenster, Wilhelm-Klemm-Strasse 9, 48149 Muenster, Germany*
[63]*University of Oxford, Keble Road, Oxford OX13RH, United Kingdom*
[64]*University of Science and Technology Liaoning, Anshan 114051, People's Republic of China*
[65]*University of Science and Technology of China, Hefei 230026, People's Republic of China*
[66]*University of South China, Hengyang 421001, People's Republic of China*
[67]*University of the Punjab, Lahore-54590, Pakistan*
[68a]*University of Turin and INFN, University of Turin, I-10125, Turin, Italy*
[68b]*University of Eastern Piedmont, I-15121, Alessandria, Italy*
[68c]*INFN, I-10125, Turin, Italy*
[69]*Uppsala University, Box 516, SE-75120 Uppsala, Sweden*
[70]*Wuhan University, Wuhan 430072, People's Republic of China*
[71]*Xinyang Normal University, Xinyang 464000, People's Republic of China*
[72]*Yunnan University, Kunming 650500, People's Republic of China*
[73]*Zhejiang University, Hangzhou 310027, People's Republic of China*
[74]*Zhengzhou University, Zhengzhou 450001, People's Republic of China*

(Received 23 December 2022; accepted 18 April 2023; published 15 May 2023)

[a]Also at the Moscow Institute of Physics and Technology, Moscow 141700, Russia.
[b]Also at the Novosibirsk State University, Novosibirsk, 630090, Russia.
[c]Also at the NRC "Kurchatov Institute," PNPI, 188300, Gatchina, Russia.
[d]Also at Goethe University Frankfurt, 60323 Frankfurt am Main, Germany.
[e]Also at Key Laboratory for Particle Physics, Astrophysics and Cosmology, Ministry of Education; Shanghai Key Laboratory for Particle Physics and Cosmology; and Institute of Nuclear and Particle Physics, Shanghai 200240, People's Republic of China.
[f]Also at Key Laboratory of Nuclear Physics and Ion-beam Application (MOE) and Institute of Modern Physics, Fudan University, Shanghai 200443, People's Republic of China.
[g]Also at State Key Laboratory of Nuclear Physics and Technology, Peking University, Beijing 100871, People's Republic of China.
[h]Also at School of Physics and Electronics, Hunan University, Changsha 410082, China.
[i]Also at Guangdong Provincial Key Laboratory of Nuclear Science, Institute of Quantum Matter, South China Normal University, Guangzhou 510006, China.
[j]Also at Frontiers Science Center for Rare Isotopes, Lanzhou University, Lanzhou 730000, People's Republic of China.
[k]Also at Lanzhou Center for Theoretical Physics, Lanzhou University, Lanzhou 730000, People's Republic of China.
[l]Also at the Department of Mathematical Sciences, IBA, Karachi, Pakistan.

Using a data sample collected with the BESIII detector operating at the BEPCII storage ring, the Born cross section of the process $e^+e^- \to \eta J/\psi$ at a center-of-mass energy $\sqrt{s} = 3.773$ GeV is measured to be $(8.88 \pm 0.87 \pm 0.42)$ pb. We fit the cross section line shape before correcting for the initial state radiation from $\sqrt{s} = 3.773$ to 4.600 GeV to obtain the branching fraction $\mathcal{B}(\psi(3770) \to \eta J/\psi)$. We obtain $\mathcal{B}(\psi(3770) \to \eta J/\psi) = (11.3 \pm 5.9 \pm 1.1) \times 10^{-4}$ when the $\psi(3770)$ decay amplitude is added coherently to the other contributions, and $(8.7 \pm 1.0 \pm 0.8) \times 10^{-4}$ when it is added incoherently. Here the quoted uncertainties are statistical and systematic, respectively. In both cases, the statistical significance of $\psi(3770)$ resonance is above $7\sigma$. This is the first time the decay $\psi(3770) \to \eta J/\psi$ is observed with a statistical significance greater than $5\sigma$.

DOI: 10.1103/PhysRevD.107.L091101

Conventionally, the $\psi(3770)$ has been regarded as the lowest-mass $D$-wave charmonium state above the $D\bar{D}$ threshold, i.e., a pure $c\bar{c}$ meson in the quark model [1]. However, this interpretation of $\psi(3770)$ results in unsolved conflicts between the standard theoretical expectations [2] and the experimental observations [3], namely, the large non-$D\bar{D}$ decay width of the state, and the abnormal ratio of the branching fractions of $\psi(3770) \to D^+D^-$ and $\psi(3770) \to D^0\bar{D}^0$. Competitive theories have been proposed to solve the puzzles, either by introducing tetraquark component into the wave function [4] or more complicated dynamics such as 2S-1D mixing between $\psi(3686)$ and $\psi(3770)$ [5–8], and re-scattering mechanism with $D$ mesons [9–12]. More experimental contributions are necessary to decide which of the existing theories is the best representation of the data or to develop a novel one.

The experimental results on the $\psi(3770)$ non-$D\bar{D}$ decays are very limited and $\psi(3770) \to \pi^+\pi^- J/\psi$ is the only well established channel [3,13]. In 2005, CLEO studied the decay $\psi(3770) \to \eta J/\psi$ [14] using data collected at the center-of-mass (c.m.) energy $\sqrt{s} = 3.773$ GeV, and the branching fraction is measured to be $\mathcal{B}(\psi(3770) \to \eta J/\psi) = (8.7 \pm 3.3 \pm 2.2) \times 10^{-4}$. The measurement was performed under the assumption of no interference between the resonant decay and the continuum process; the statistical significance is of $3.5\sigma$. The branching fraction of $\psi(3770) \to \eta J/\psi$ is utilized as an input in theoretical calculations of decay properties not only for conventional charmonium states [15,16] but also for exotic charmoniumlike (also called $XYZ$) states [17] observed in this energy region. Recently, BESIII reported evidence for $e^+e^- \to \pi^+\pi^-\psi(3770)$ at $\sqrt{s} = 4.26$ and 4.36 GeV [18], indicating a possible link between the $\psi(3770)$ and the charmoniumlike states $Y(4260)$ and $Y(4360)$ [19–23]. In order to improve our knowledge of the nature of $\psi(3770)$ and its decay mechanism, it is desirable to obtain a more precise measurement with proper consideration of the possible interference between the resonant decay and the continuum process. This will also deepen the understanding of the nature of the $XYZ$ states and—more generally—the nonperturbative behavior of the strong interaction.

In this paper, we report the measurement of the Born cross section of $e^+e^- \to \eta J/\psi$ using 2.93 fb$^{-1}$ of data [24] taken at $\sqrt{s} = 3.773$ GeV with the BESIII detector. The branching fraction $\mathcal{B}(\psi(3770) \to \eta J/\psi)$ is determined by fitting the cross-section line-shape before correcting for initial state radiation (dressed cross section) and by incorporating previous measurements [25]. The $J/\psi$ is reconstructed through its decay to dimuons. The dielectron decay is not used because of the high contamination from the radiative Bhabha process.

The BESIII detector is a magnetic spectrometer [26] located at the Beijing Electron Positron Collider (BEPCII). The cylindrical core of the BESIII detector consists of a helium-based multilayer drift chamber (MDC), a plastic scintillator time-of-flight system (TOF), and a CsI (Tl) electromagnetic calorimeter (EMC), which are all enclosed in a superconducting solenoidal magnet providing a 1.0 T magnetic field. The solenoid is supported by an octagonal flux-return yoke with resistive plate counter muon identifier modules interleaved with steel. The acceptance of charged particles and photons is 93% over $4\pi$ solid angle. The charged-particle momentum resolution at 1 GeV$/c$ is 0.5%, and the specific ionization energy loss resolution is 6% for the electrons from Bhabha scattering. The EMC measures photon energies with a resolution of 2.5% (5%) at 1 GeV in the barrel (endcap) region. The time resolution of the TOF barrel part is 68 ps, while that of the endcap part is 110 ps.

Large samples of simulated events produced with the GEANT4 based [27] Monte Carlo (MC) software, which includes the geometric description of the BESIII detector and the detector response, are used to determine the detection efficiency and to estimate the background contribution. The simulation includes the beam-energy spread and initial state radiation (ISR) in the $e^+e^-$ annihilations modeled with the generator KKMC [28,29]. The decays $\psi(3770) \to J/\psi\eta$, $J/\psi \to \mu^+\mu^-$, and $\eta \to \gamma\gamma$ are generated with the HELAMP (helicity amplitude), VLL (vector lepton lepton), and phase space configurations of EvtGen [30,31], respectively. The inclusive MC samples consist of the production of the $D\bar{D}$ pairs, the non-$D\bar{D}$ decays of the $\psi(3770)$, the ISR production of $J/\psi$ and $\psi(3686)$ states, and the continuum processes ($e^+e^- \to u\bar{u}, d\bar{d}, s\bar{s}$) incorporated in KKMC [28,29]. The known decay modes are modeled with EvtGen [30,31] using branching fractions taken from the Particle Data Group (PDG) [3], and the remaining unknown decays from the charmonium states with LUNDCHARM [32,33]. The final-state radiation from charged particles is incorporated with the PHOTOS package [34].

Each candidate event is required to have two charged tracks with zero net charge, and at least two photon candidates. For each charged track, the distance of the closest approach to the interaction point is required to be less than 1 cm in the radial direction and less than 10 cm along the beam axis. The polar angle $\theta$ of the tracks with respect to the axis of the MDC must be within the fiducial volume of the MDC ($|\cos\theta| < 0.93$). Photon candidates are reconstructed from isolated showers in the EMC which are at least 10° away from the nearest charged track. The photon energy is required to be at least 25 MeV in the barrel region ($|\cos\theta| < 0.80$) or 50 MeV in the endcap region ($0.86 < |\cos\theta| < 0.92$). In order to suppress electronic noise and energy depositions which are unrelated to the event, the difference between the EMC time and the event start time is required to satisfy $0 \le t \le 700$ ns.

Tracks with momentum greater than 1 GeV/$c$ and energy deposited in the EMC less than 0.4 GeV are assumed to be muon candidates from $J/\psi$ decay. A vertex fit is performed for the two charged tracks, constraining them to originate from the interaction point. To improve the resolution and suppress background, a four-constraint (4C) kinematic fit is applied for the candidate events, imposing energy-momentum conservation under the hypothesis of $e^+e^- \to \gamma\gamma\mu^+\mu^-$. In the case the event has more than two photon candidates, all photon pairs are tested in the kinematic fit and the combination with the smallest value of $\chi^2_{4C}$ is retained. The events are required to satisfy $\chi^2_{4C} < 48$ to be retained for further analysis. This requirement is set by optimizing a figure-of-merit, defined as $\frac{S}{\sqrt{S+B}}$, where $S$ is the number of signal MC events and $B$ is the number of background events from the inclusive MC samples. The values of $S$ and $B$ are normalized according to the integrated luminosity and the branching fraction of $\psi(3770) \to \eta J/\psi$ from the CLEO measurement [14]. To further suppress background events, the higher and lower energy photons are required to satisfy $E_{\gamma\mathrm{high}} < 0.52$ GeV and $E_{\gamma\mathrm{low}} > 0.135$ GeV, respectively. To remove contamination from the background process $\psi(3770) \to \gamma\chi_{c1}, \chi_{c1} \to \gamma J/\psi, J/\psi \to \mu^+\mu^-$, any event with $0.239~\mathrm{GeV} < E_{\gamma\mathrm{low}} < 0.259$ GeV and $0.377~\mathrm{GeV} < E_{\gamma\mathrm{high}} < 0.396$ GeV is removed.

Figure 1 presents the distribution of the modified invariant mass of the $\gamma\gamma$ pair [$M'(\gamma\gamma)$] against the invariant mass of the $\mu^+\mu^-$ pair [$M(\mu\mu)$] for the events in data after applying all the selection criteria. Here $M'(\gamma\gamma) \equiv M(\gamma\gamma) + M(\mu\mu) - m_{J/\psi}$, where $m_{J/\psi}$ is the known $J/\psi$ mass [3]. A clear accumulation of signal is observed around the intersection of the $J/\psi$ and $\eta$ mass regions.

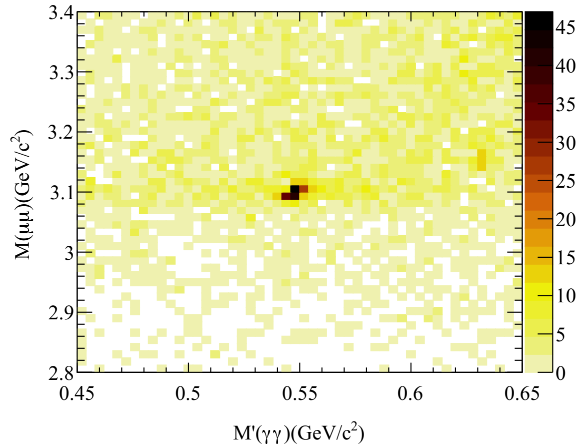


FIG. 1. Distribution of $M'(\gamma\gamma)$ versus $M(\mu\mu)$ of the candidate events for $e^+e^- \to \eta J/\psi$ in data.

The number of signal events is obtained by an unbinned maximum-likelihood fit to the distributions of $M'(\gamma\gamma)$ in the $J/\psi$ signal region and sideband regions, with the $\eta$ signal line-shape shared for both regions. The $J/\psi$ signal region is defined as $M(\mu\mu) \in (3.06, 3.15)$ GeV/$c^2$ and the sideband regions as $M(\mu\mu) \in (2.9, 3.0)$ GeV/$c^2$ and $(3.2, 3.3)$ GeV/$c^2$. The $\eta$ signal is described by the sum of a Crystal Ball function [35] and a Gaussian function, while the combinatorial background is described by a second-order polynomial function. The number of $\eta$ events in the sideband regions is multiplied by a scale factor $f$ and subtracted from the number of $\eta$ event in the signal region, to give the signal yield. The scale factor $f = 0.49$ is the ratio of non-$J/\psi$ events in the $J/\psi$ signal region and sideband regions, determined by a fit to the $M(\mu\mu)$ distribution. In the fit, the $J/\psi$ signal is described by the shape extracted from the signal MC simulation and the combinatorial background is described by a third-order Chebychev polynomial function. Figure 2 shows the distributions and fit results in $M(\mu\mu)$ and $M'(\gamma\gamma)$. The observed signal yield is determined to be $N^{\mathrm{obs}} = 232 \pm 23$, where the uncertainty is statistical only.

The Born cross section is determined by

$$\sigma^B(e^+e^- \to \eta J/\psi) = \frac{N^{\mathrm{obs}}}{\mathcal{L} \cdot (1+\delta^{\mathrm{ISR}}) \cdot (1+\delta^{\mathrm{VP}}) \cdot \varepsilon \cdot \mathcal{B}r}, \quad (1)$$

where $\mathcal{L}$ is the integrated luminosity, $(1+\delta^{\mathrm{ISR}})$ is the ISR correction factor [36], $(1+\delta^{\mathrm{VP}})$ is the vacuum polarization factor taken from QED calculation [37], $\mathcal{B}r$ is the product of the branching fractions of the subsequent decays of intermediate states as given by the PDG [3], and $\varepsilon$ is the detection efficiency. The ISR correction factor is obtained by an iterative method [38], in which the dressed cross section

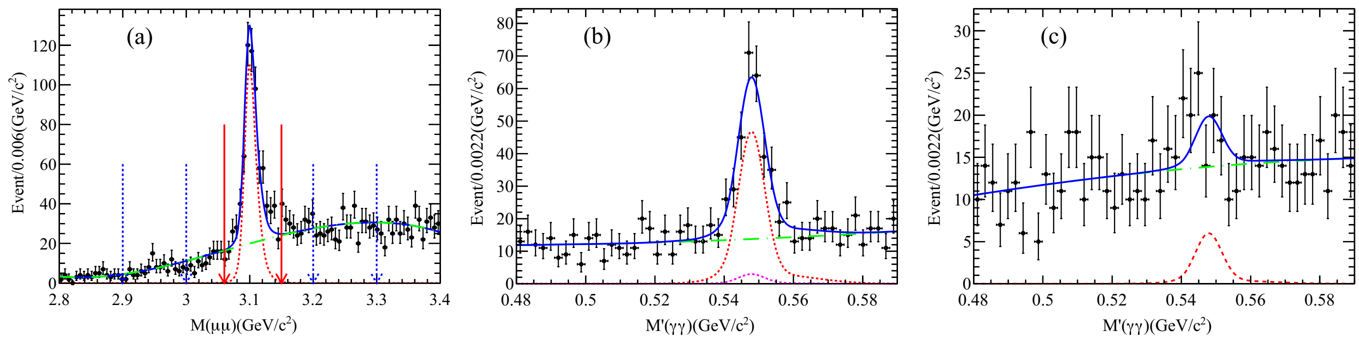


FIG. 2. Distribution of $M(\mu\mu)$ from data (a). The signal region is defined as the mass region between the two red arrows, while the two sideband regions are defined as the ranges between the blue arrows. Distributions of $M'(\gamma\gamma)$ in the $J/\psi$ signal region (b) and sideband regions (c). The $M'(\gamma\gamma)$ component in the $J/\psi$ sidebands is also shown in (b) (pink curve). The points with error bars are data, the blue solid curves represent the fit results, the red dashed curves represent signals components, and the green dot-dashed curves represent background components.

of $e^+e^- \to \eta J/\psi$ measured in this study and previously with c.m. energies from $\sqrt{s} = 3.81$ to 4.60 GeV [25] are used as input. Table I shows the measured Born cross section at $\sqrt{s} = 3.773$ GeV and the values of the other parameters in Eq. (1).

The following sources of the systematic uncertainty are considered in the cross-section measurement. The uncertainty on the integrated luminosity is 0.5% [24]. The uncertainty associated with the reconstruction efficiency of an individual lepton or photon is 1.0% [39–41], giving 2% for each pair of particles. An uncertainty of 1% associated with the $J/\psi$ mass window requirement is assigned by comparing the $J/\psi$ mass resolution between data and MC simulation, and taking the difference in the selection efficiency. The helix parameters of the charged tracks are corrected in simulation to improve the agreement of $\chi^2_{4C}$ between data and MC simulation [42]; the systematic uncertainty from the kinematic fit is estimated by removing the correction and taking the 0.6% difference in the detection efficiency as the uncertainty. The systematic uncertainty from the ISR correction factor associated with the input cross section line-shape is estimated by sampling the parameters of the dressed cross-section line shape using a multidimensional Gaussian function. The resultant distribution of $(1+\delta^{\rm ISR})$ values is fitted with a Gaussian function and the standard deviation of 0.5% is assigned as the systematic uncertainty. In addition, the $\psi(3770)$ and $\psi(4040)$ resonance parameters are varied within their uncertainties and the parametrization of the continuum is considered by changing the $1/s$ cross-section dependence to $1/s^n$ with $n$ as a free parameter, giving a 2.3% uncertainty. The uncertainties on the quoted branching fractions of the decays of the intermediate states are taken from the PDG [3], and lead to a 0.8% uncertainty on the cross section. To determine the uncertainty associated with the fit procedure, we perform alternative fits by varying the resolution of the signal shape, the order of the polynomial background shape, the normalization factor, and the fit range, individually, and use the difference in results to assign a 2.0% uncertainty. The total systematic uncertainty is obtained to be 4.7% adding all the individual items in quadrature, where the dominant contribution is from the background shape. The systematic uncertainty from each source is given in Table II.

The branching fraction of $\psi(3770) \to \eta J/\psi$ is determined from a maximum likelihood fit to the dressed cross section of $e^+e^- \to \eta J/\psi$ from $\sqrt{s} = 3.773$ to 4.6 GeV. The likelihood is constructed taking the fluctuations of the number of signal and background events into account [43]. Two scenarios are used to describe the dressed cross section line-shape, with two different treatments of the $\psi(3770)$ resonant decay amplitude: one, in which the $\psi(3770)$ amplitude is coherent with the other amplitudes considered, and one where it is added incoherently.

$$\sigma_{\rm co} = |C\cdot\sqrt{\Phi(s)} + e^{i\phi_1}{\rm BW}_{\psi(3770)} + e^{i\phi_2}{\rm BW}_{\psi(4040)} + e^{i\phi_3}{\rm BW}_{Y(4230)} + e^{i\phi_4}{\rm BW}_{Y(4390)}|^2, \quad (2)$$

TABLE I. The values of the integrated luminosity $\mathcal{L}$, the detection efficiency $\varepsilon$, the product of radiative correction factor and vacuum polarization factor $(1+\delta^{\rm ISR})\cdot(1+\delta^{VP})$, and the obtained Born cross section of $e^+e^- \to \eta J/\psi$ at $\sqrt{s} = 3.773$ GeV. The uncertainties on the efficiency and cross section are statistical only.

| $\mathcal{L}$ (pb$^{-1}$) | $\varepsilon$(%) | $(1+\delta^{\rm ISR})\cdot(1+\delta^{VP})$ | $\mathcal{B}(J/\psi\to\mu^+\mu^-)$(%) | $\mathcal{B}(\eta\to\gamma\gamma)$(%) | $N^{\rm obs}$ | $\sigma^B$(pb) |
|---|---|---|---|---|---|---|
| $2931\pm15$ | $47.8\pm0.1$ | 0.79 | $5.96\pm0.03$ | $39.4\pm0.2$ | $232\pm23$ | $8.88\pm0.87$ |

TABLE II. Systematic uncertainties on the Born cross section of $e^+e^- \to \eta J/\psi$ at $\sqrt{s} = 3.773$ GeV.

| Source | Uncertainty (%) |
|---|---|
| Luminosity* | 0.5 |
| Photon detection* | 2.0 |
| Tracking efficiency* | 2.0 |
| Lepton-pair mass window | 1.0 |
| 4C kinematic fit | 0.6 |
| Background shape | 2.3 |
| Fit range | 2.0 |
| Signal shape | 1.5 |
| Radiative correction | 0.5 |
| Quoted branching fractions* | 0.8 |
| Total | 4.7 |

The contributions marked with * are common for all center-of-mass energies.

$$\sigma_{\rm inco} = |{\rm BW}_{\psi(3770)}|^2 + |C \cdot \sqrt{\Phi(s)} + e^{i\phi_2}{\rm BW}_{\psi(4040)} + e^{i\phi_3}{\rm BW}_{Y(4230)} + e^{i\phi_4}{\rm BW}_{Y(4390)}|^2. \quad (3)$$

Here $\Phi(s) = q^3/s$ is the $P$-wave phase space factor used to parametrize the continuum term, with $q$ being the $\eta$ momentum in the $e^+e^-$ c.m. frame, ${\rm BW} = \frac{\sqrt{12\pi\mathcal{B}\Gamma_{ee}\Gamma}}{s-M^2+iM\Gamma}\sqrt{\frac{\Phi(s)}{\Phi(M^2)}}$ is the Breit-Wigner function, $\phi$ is the relative phase between the resonant decay and the phase space term, and $C$ is a real parameter. In the Breit-Wigner formula, $M$, $\Gamma$, and $\Gamma_{ee}$ and $\mathcal{B}$ are the mass, the total width, the electronic width (whose definition includes vacuum polarization effects), and the branching fraction to $\eta J/\psi$ of the resonance. The mass and total width of $\psi(3770)$ and $\psi(4040)$, and the electronic width of $\psi(3770)$ are fixed to the PDG values [3], while $\mathcal{B}$ and the parameters of the other resonances are free parameters to be determined by the fit. Only the statistical uncertainty of the dressed cross section is considered in the fit. There are four solutions from the coherent fit and one solution from the incoherent fit. The fit results are summarized in Table III. Figure 3 shows the cross-section measurements plotted against $\sqrt{s}$, with the fit results superimposed. The result for the coherent fit is degenerate for the four solutions. The fit qualities estimated by a $\chi^2$-test approach are $\chi^2/\text{n.d.f.} = 88.1/119$ for the coherent fit and $92.2/120$ for the incoherent fit, where n.d.f is the number of degrees of freedom. The statistical significance of the $\psi(3770) \to \eta J/\psi$ decay in the coherent (incoherent) fit is estimated to be $7.9\sigma$ ($8.3\sigma$), calculated by the change of the likelihood values with and without the $\psi(3770)$ resonance contribution included, and taking the change in the number of degrees of freedom into account [44]. The branching fractions from the fits of the other resonant parameters are consistent with those found in the earlier study [25]. The statistical uncertainty on the fit assuming coherence among all amplitudes is large due to the lack of data points around the $\psi(3770)$ peak, and this leads to a poor constraint on the relative phase $\phi_1$.

There are several sources of potential systematic bias in the branching-fraction measurement. By way of example, we quote the uncertainties for solution 1 of the coherent fit. The uncertainty of the c.m. energy is 0.8 MeV [45] for all data samples; this uncertainty is propagated to the branching-fraction measurement to give a relative uncertainty of 0.5%. The uncertainty from the energy spread is 0.1%, which is estimated by convolving the fit formula with a Gaussian function with a standard deviation of 1.4 MeV, which is the measured value of the spread [43,46]. The uncertainty arising from the $\psi(3770)$ and $\psi(4040)$ resonant parameters is studied by varying the parameters within their uncertainties, which leads to an effect of 8.1%, where the dominant contribution (6.9%) is from the partial width to dielectrons. The uncertainty of the parameterization of the continuum term (0.8%) is considered by changing the $1/s$ dependence to $1/s^n$, where $n$ is a free parameter. The uncertainty from the dressed cross-section measurement has a contribution that is uncorrelated among the c.m. energy points and a contribution that is common to all data points. The uncorrelated uncertainty of 1.7% is included in the fit to the dressed cross section; the correlated uncertainty of 3.0% is propagated to the $\mathcal{B}(\psi(3770) \to \eta J/\psi)$ measurement. The total systematic uncertainty is 8.9%, and the individual contributions are listed in Table IV.

In summary we measure the Born cross section of $e^+e^- \to \eta J/\psi$ at $\sqrt{s} = 3.773$ GeV using 2.93 fb$^{-1}$

TABLE III. Fitting results of the $e^+e^- \to \eta J/\psi$ decay. The uncertainties on the branching fractions and $\phi$ are statistical and systematic. The $C_0$ of the four solutions in the coherent fit are the same.

| Parameters | Coherent fit | | | | Incoherent fit |
|---|---|---|---|---|---|
| | Solution1 | Solution2 | Solution3 | Solution4 | |
| $M_1$(MeV/$c^2$) | 3773.7 (fixed) | | | | 3773.7 (fixed) |
| $\Gamma_1$(MeV) | 27.2 (fixed) | | | | 27.2 (fixed) |
| $C_0$ | $13.3 \pm 1.9$ | | | | $11.0 \pm 1.6$ |
| $\mathcal{B}r_1$($\times 10^{-4}$) | $11.3 \pm 5.9 \pm 1.1$ | $11.6 \pm 6.0 \pm 1.1$ | $11.2 \pm 5.8 \pm 1.1$ | $11.5 \pm 6.0 \pm 1.1$ | $8.7 \pm 1.0 \pm 0.8$ |
| $\phi_1$(rad) | $3.9 \pm 0.6 \pm 0.07$ | $4.2 \pm 0.6 \pm 0.09$ | $3.7 \pm 0.6 \pm 0.05$ | $4.1 \pm 0.6 \pm 0.08$ | |

electron-positron annihilation data collected with the BESIII detector. The cross section is measured to be $\sigma^B(e^+e^- \to \eta J/\psi) = (8.88 \pm 0.87_{\rm stat} \pm 0.42_{\rm sys})$ pb. The branching fraction of $\psi(3770) \to \eta J/\psi$ is determined from the fit to the cross section line-shape of $e^+e^- \to \eta J/\psi$ in the range of $\sqrt{s} = 3.773$ to 4.60 GeV including the decays of the $\psi(3770)$, $\psi(4040)$, $Y(4230)$, and $Y(4390)$ resonances as well as the phase space term. When the interference of the decay of the $\psi(3770)$ with the other processes is neglected, the branching fraction is determined to be $(8.7 \pm 1.0_{\rm stat} \pm 0.8_{\rm sys}) \times 10^{-4}$, which is close to the result of CLEO [14] but with triple the precision. When interference is considered, four solutions are obtained with branching fractions varying between $(11.2 \pm 5.8_{\rm stat} \pm 1.1_{\rm sys}) \times 10^{-4}$ and $(11.6 \pm 6.0_{\rm stat} \pm 1.1_{\rm sys}) \times 10^{-4}$. The statistical significance of the $\psi(3770)$ resonance contribution is $8.3\sigma$ and $7.9\sigma$ for the two fit assumptions. The difference in the branching fractions reflects that there exists substantial interference effect, especially the unexpected interference between $\psi(3770)$ and highly excited vector charmonium(like) states. This interference effect has been ignored in previous experimental measurements [14,47–49]

This measurement of $\psi(3770) \to \eta J/\psi$ is a new contribution to the knowledge of $\psi(3770)$ non-$D\bar{D}$ decays. These results will improve the calculations as essential input, to the calculations of charmonia decaying into light vector pseudo-scalar (VP) states [15,16] and hadronic transitions of highly excited charmonium(like) states [17]. Although the measured branching fraction is close to the predicted value of Ref. [4] and hint at a possible tetraquark component in the $\psi(3770)$ resonance, no firm conclusion can be made on this matter at present. Improved measurements of $\psi(3770) \to \pi^+\pi^- J/\psi$, $\pi^0 J/\psi$, $\gamma\chi_{cJ}$, etc., in the future, as well as a finer scan around the $\psi(3770)$ are desirable to reveal the nature of this resonance.

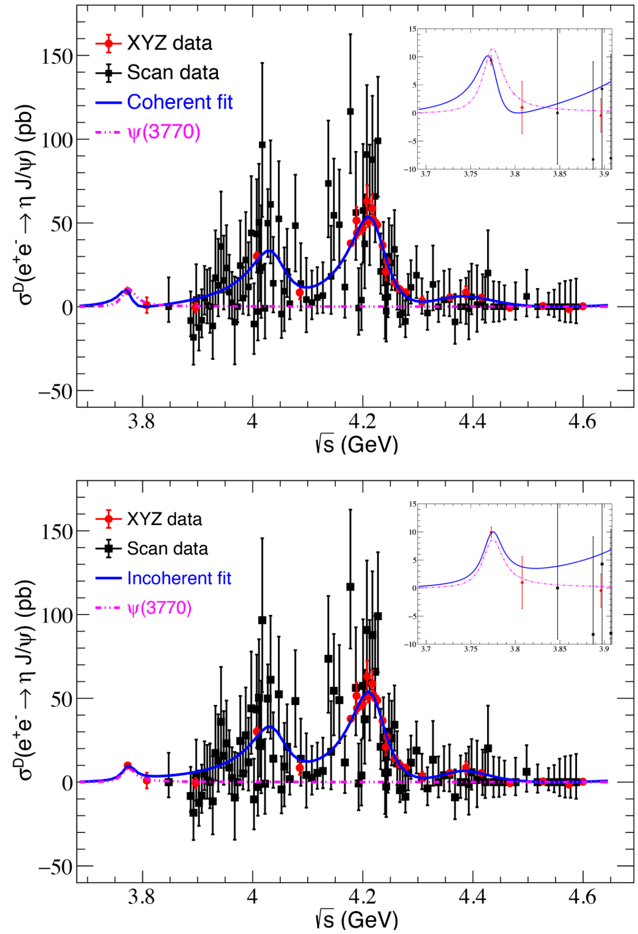


FIG. 3. Top: coherent and bottom: incoherent fits to the dressed cross section line-shape of $e^+e^- \to \eta J/\psi$. The points with error bars are data and the solid curves are the best fit results. The insert is the zoomed distribution in the $\psi(3770)$ mass region.

The BESIII collaboration thanks the staff of BEPCII and the IHEP computing center for their strong support.

TABLE IV. Relative systematic uncertainties in percent on the branching fraction of $\psi(3770) \to \eta J/\psi$.

| | Coherent fit | | | | | | | | |
|---|---|---|---|---|---|---|---|---|---|
| | Solution1 | | Solution2 | | Solution3 | | Solution4 | | Incoherent fit |
| Source | $Br$ | $\phi$ | $Br$ | $\phi$ | $Br$ | $\phi$ | $Br$ | $\phi$ | $Br$ |
| Center-of-mass energy | 3.3 | 0.2 | 3.5 | 0.1 | 3.4 | 0.1 | 3.2 | 0.2 | 2.1 |
| Energy spread | 0.8 | 0.1 | 0.9 | 0.1 | 0.9 | 0.1 | 0.8 | 0.1 | 1.0 |
| $\psi(3770)$ mass | 1.5 | 0.1 | 1.4 | 0.1 | 1.5 | 0.1 | 1.4 | 0.1 | 0.9 |
| $\psi(3770)$ width | 4.2 | 0.1 | 4.2 | 0.1 | 4.1 | 0.1 | 4.1 | 0.1 | 3.6 |
| $\psi(3770)\Gamma_{e^+e^-}$ | 6.9 | | 6.9 | | 6.9 | | 6.9 | | 6.9 |
| $\psi(4040)$ mass | 0.5 | 0.4 | 0.2 | 0.1 | 0.4 | 0.3 | 0.3 | 0.1 | 0.4 |
| $\psi(4040)$ width | 0.7 | 0.3 | 1.0 | 0.8 | 1.1 | 0.5 | 0.8 | 0.8 | 0.7 |
| Continuum term | 0.9 | 1.8 | 0.9 | 2.0 | 0.9 | 1.3 | 1.0 | 1.6 | 1.3 |
| Correlated systematic uncertainties | 3.0 | | 3.0 | | 3.0 | | 3.0 | | 3.0 |
| Uncorrelated systematic uncertainties | 0.2 | 0.1 | 0.1 | 0.1 | 0.1 | 0.1 | 2.0 | 0.5 | 0.1 |
| Total | 9.5 | 1.9 | 9.5 | 2.2 | 9.5 | 1.4 | 9.6 | 1.9 | 8.8 |

This work is supported in part by National Key Research and Development Program of China under Contracts No. 2020YFA0406300, No. 2020YFA0406400; National Natural Science Foundation of China (NSFC) under Contracts No. 11625523, No. 11635010, No. 11735014, No. 11822506, No. 11835012, No. 11935015, No. 11935016, No. 11935018, No. 11961141012, No. 12022510, No. 12025502, No. 12035009, No. 12035013, No. 12061131003; The key scientific research Projects of colleges and universities in Henan Province (21A140012); the Chinese Academy of Sciences (CAS) Large-Scale Scientific Facility Program; Joint Large-Scale Scientific Facility Funds of the NSFC and CAS under Contracts No. U1732263, No. U1832207, No. U2032108; CAS Key Research Program of Frontier Sciences under Contract No. QYZDJ-SSW-SLH040; the CAS Center for Excellence in Particle Physics (CCEPP); 100 Talents Program of CAS; INPAC and Shanghai Key Laboratory for Particle Physics and Cosmology; ERC under Contract No. 758462; European Union Horizon 2020 research and innovation programme under Contract No. Marie Sklodowska-Curie grant agreement No. 894790; German Research Foundation DFG under Contracts No. 443159800, Collaborative Research Center CRC 1044, FOR 2359, GRK 2149; Istituto Nazionale di Fisica Nucleare, Italy; Ministry of Development of Turkey under Contract No. DPT2006K-120470; National Science and Technology fund; Olle Engkvist Foundation under Contract No. 200-0605; STFC (United Kingdom); The Knut and Alice Wallenberg Foundation (Sweden) under Contract No. 2016.0157; The Royal Society, UK under Contracts No. DH140054, No. DH160214; The Swedish Research Council; U.S. Department of Energy under Contracts No. DE-FG02-05ER41374, No. DE-SC-0012069.

---

[1] E. Eichten, K. Gottfried, T. Kinoshita, K. D. Lane, and T. M. Yan, Phys. Rev. D **17**, 3090 (1978).
[2] Z. G. He, Y. Fan, and K. T. Chao, Phys. Rev. Lett. **101**, 112001 (2008).
[3] R. L. Workman *et al.* (Particle Data Group), Prog. Theor. Exp. Phys. **2022**, 083C01 (2022).
[4] M. B. Voloshin, Phys. Rev. D **71**, 114003 (2005).
[5] X. H. Mo, C. Z. Yuan, and P. Wang, Chin. Phys. C **31**, 686 (2007), http://hepnp.ihep.ac.cn//article/id/d7f266c1-9574-470c-9a0d-c9da20a5a2e2.
[6] J. L. Rosner, Ann. Phys. (Amsterdam) **319**, 1 (2005).
[7] Y. J. Zhang and Q. Zhao, Phys. Rev. D **81**, 034011 (2010).
[8] Y. B. Ding, D. H. Qin, and K. T. Chao, Phys. Rev. D **44**, 3562 (1991).
[9] Z. k. Guo, S. Narison, J. M. Richard, and Q. Zhao, Phys. Rev. D **85**, 114007 (2012).
[10] Q. Wang, X. H. Liu, and Q. Zhao, Phys. Rev. D **84**, 014007 (2011).
[11] X. Liu, B. Zhang, and X. Q. Li, Phys. Lett. B **675**, 441 (2009).
[12] F. K. Guo, C. Hanhart, G. Li, U. G. Meissner, and Q. Zhao, Phys. Rev. D **83**, 034013 (2011).
[13] E. Eichten, S. Godfrey, H. Mahlke, and J. L. Rosner, Rev. Mod. Phys. **80**, 1161 (2008).
[14] N. E. Adam *et al.* (CLEO Collaboration), Phys. Rev. Lett. **96**, 082004 (2006).
[15] Y. J. Zhang, G. Li, and Q. Zhao, Phys. Rev. Lett. **102**, 172001 (2009).
[16] G. Li, X. h. Liu, Q. Wang, and Q. Zhao, Phys. Rev. D **88**, 014010 (2013).
[17] M. N. Anwar, Y. Lu, and B. S. Zou, Phys. Rev. D **95**, 114031 (2017).
[18] M. Ablikim *et al.* (BESIII Collaboration), Phys. Rev. D **100**, 032005 (2019).
[19] L. Maiani, V. Riquer, F. Piccinini, and A. D. Polosa, Phys. Rev. D **72**, 031502 (2005).
[20] H. X. Chen, W. Chen, X. Liu, and S. L. Zhu, Phys. Rep. **639**, 1 (2016).
[21] S. L. Olsen, T. Skwarnicki, and D. Zieminska, Rev. Mod. Phys. **90**, 015003 (2018).
[22] N. Brambilla, S. Eidelman, C. Hanhart, A. Nefediev, C. P. Shen, C. E. Thomas, A. Vairo, and C. Z. Yuan, Phys. Rep. **873**, 1 (2020).
[23] K. Zhu, Int. J. Mod. Phys. A **36**, 2150126 (2021).
[24] M. Ablikim *et al.* (BESIII Collaboration), Chin. Phys. C **42**, 063001 (2018).
[25] M. Ablikim *et al.* (BESIII Collaboration), Phys. Rev. D **102**, 031101 (2020).
[26] M. Ablikim *et al.* (BESIII Collaboration), Nucl. Instrum. Methods Phys. Res., Sect. A **614**, 345 (2010).
[27] S. Agostinelli *et al.* (GEANT4 Collaboration), Nucl. Instrum. Methods Phys. Res., Sect. A **506**, 250 (2003).
[28] S. Jadach, B. F. L. Ward, and Z. Was, Phys. Rev. D **63**, 113009 (2001).
[29] S. Jadach, B. F. L. Ward, and Z. Was, Comput. Phys. Commun. **130**, 260 (2000).
[30] D. J. Lange, Nucl. Instrum. Methods Phys. Res., Sect. A **462**, 152 (2001).
[31] R. G. Ping, Chin. Phys. C **32**, 599 (2008).
[32] J. C. Chen, G. S. Huang, X. R. Qi, D. H. Zhang, and Y. S. Zhu, Phys. Rev. D **62**, 034003 (2000).
[33] R. L. Yang, R. G. Ping, and H. Chen, Chin. Phys. Lett. **31**, 061301 (2014).
[34] E. Barberio and Z. Was, Comput. Phys. Commun. **79**, 291 (1994).
[35] J. Gaiser, E. D. Bloom, F. Bulos, G. Godfrey, C. M. Kiesling, W. S. Lockman, M. Oreglia, D. L. Scharre, C. Edwards, R. Partridge *et al.*, Phys. Rev. D **34**, 711 (1986).

[36] E. A. Kuraev and V. S. Fadin, Sov. J. Nucl. Phys. **41**, 466 (1985).
[37] S. Actis *et al.*, Eur. Phys. J. C **66**, 585 (2010).
[38] W. Sun, T. Liu, M. Jing, L. Wang, B. Zhong, and W. Song, Front. Phys. (Beijing) **16**, 64501 (2021).
[39] M. Ablikim *et al.* (BESIII Collaboration), Phys. Rev. Lett. **110**, 252001 (2013).
[40] M. Ablikim *et al.* (BESIII Collaboration), Phys. Rev. D **86**, 071101 (2012).
[41] M. Ablikim *et al.* (BESIII Collaboration), Phys. Rev. D **91**, 112005 (2015).
[42] M. Ablikim *et al.* (BESIII Collaboration), Phys. Rev. D **87**, 012002 (2013).
[43] M. Ablikim *et al.* (BESIII Collaboration), Phys. Rev. Lett. **118**, 092002 (2017).
[44] S. S. Wilks, Ann. Math. Stat. **9**, 60 (1938).
[45] M. Ablikim *et al.* (BESIII Collaboration), Phys. Rev. Lett. **118**, 092001 (2017).
[46] E. V. Abakumova *et al.*, Nucl. Instrum. Methods Phys. Res., Sect. A **659**, 21 (2011).
[47] J. Z. Bai *et al.* (BES Collaboration), Phys. Lett. B **605**, 63 (2005).
[48] T. E. Coan *et al.* (CLEO Collaboration), Phys. Rev. Lett. **96**, 182002 (2006).
[49] R. A. Briere *et al.* (CLEO Collaboration), Phys. Rev. D **74**, 031106 (2006).